E-proceedings of the 36th IAHR World Congress
28 June – 3 July, 2015, The Hague, the Netherlands

SECONDARY FLOW IN SHARP OPEN-CHANNEL BENDS: EXPERIMENTS AND MODELING

KOEN BLANCKAERT[1,2], MIAO WEI[1,2], JORIS HEYMAN[3], DANXUN LI[2] & ANTON J. SCHLEISS[1]

[1] *Laboratory of Hydraulic Constructions, ENAC, EPFL, Lausanne, Switzerland, koen.blanckaert@epfl.ch, anton.schleiss@epfl.ch*

[2] *State Key Laboratory of Hydroscience and Engineering, Tsinghua University, Beijing, China, miaowei12358@126.com, lidx@mail.tsinghua.edu.cn*

[3] *Environmental Hydraulics Laboratory, ENAC, EPFL, Lausanne, Switzerland, joris.heyman@epfl.ch*

ABSTRACT

The dependence of curvature-induced secondary flow on the curvature ratio *H/R* and the Froude number *Fr* was systematically investigated in a series of 18 experiments in a sharply-curved laboratory flume. The investigated flow depths were 0.9 m, 0.13 m, 0.19 m and 0.26 m, resulting in *H/R* values of 0.053, 0.077, 0.112 and 0.153, and the Froude numbers were 0.1, 0.2, 0.3, 0.4 and 0.5. The normalized magnitude of the secondary flow did not increase with *H/R*, as predicted by commonly used parameterizations for secondary flow, but remained quasi-constant. This confirms observations by Blanckaert (2009), who called this phenomenon the saturation of the secondary flow. The experiments did not reveal any dependence of the secondary flow on *Fr*. Predictions of the magnitude of the secondary flow with the nonlinear model of Blanckaert and de Vriend ((2003, 2010) agreed very well with the experimental data.

Keywords: Secondary flow, curvature, sharp bend, experiments, theoretical model

1. INTRODUCTION

Flow in curved open-channel reaches follows a helicoidal path. Secondary flow is defined as the flow component perpendicular to the channel axis in the present paper. Secondary flow induced by the streamline curvature is known to redistribute mass, momentum, boundary shear stress, and sediment transport, and thereby plays an important role with respect to the water quality, velocity distribution, and river morphology. Since the first investigations of Fargue (1868) and Thomson (1876), curvature-induced secondary flow has been abundantly investigated by means of field measurements, laboratory measurements, analytical modeling and numerical modeling. We refer to Blanckaert & de Vriend (2004) for a literature review. Nevertheless, there are still open questions with respect to the physics and the numerical modeling of secondary flow, especially in sharply curved channel reaches.

In mildly and moderately curved channel reaches, the curvature-induced secondary flow is known to scale with the ratio of flow depth to centerline radius of curvature, *H/R*, i.e. the magnitude of the secondary flow increases linearly with curvature ratio *H/R*. Therefore, the transverse component of the secondary flow is often represented as:

$$v_n^* = v_n - U_n = U \frac{H}{R} f_n \tag{1}$$

where v_n is the transverse component of the velocity vector, U_n the depth-averaged transverse velocity, , and f_n a function that represents the normalized vertical profile of v_n^*. The magnitude of the secondary flow can be quantified by:

$$\sqrt{\left\langle v_n^{*,2} \right\rangle} = U \frac{H}{R} \sqrt{\left\langle f_n^2 \right\rangle} \tag{2}$$

where $\langle \ \rangle$ is the depth-averaging operator. In sharply curved reaches, however, the secondary flow seems to reach a maximum value that is independent of *H/R*, i.e. a further increase in *H/R* does not lead to an increase in secondary flow magnitude. Blanckaert (2009) has termed this phenomenon the saturation of the secondary flow. Understanding of secondary flow in sharply curved reaches is still hampered by the paucity of experimental data.

Three-dimensional numerical models directly resolve the curvature-induced secondary flow. But the application range of these models is still limited to problems on a relatively small spatial and short temporal scale. Large-scale and long-term problems are commonly investigated with depth-averaged or cross-sectional-averaged numerical models, which are inherently unable to resolve secondary flow. An adequate parameterization of the secondary flow does allow, however, accounting for the effects of secondary flow on the flow field in these reduced-order models. Previously proposed parameterizations were all limited to mild and moderately curved reaches (van Bendegom 1947, Rozovskii 1957, Engelund 1974, de Vriend 1977, Johannesson & Parker 1989, etc). These parameterizations describe the transverse component of the curvature-induced secondary flow v_n^* as:

$$v_{n,0}^{*} = v_n - U_n = U\frac{H}{R} f_{n,0}(C_f) \tag{3}$$

where the function $f_{n,0}$ uniquely depend on the dimensionless Chézy friction coefficient C_f. Because $v_{n,0}^{*}$ increases linearly with *H/R*, these parameterizations are called linear models, and indicated with the index 0. Blanckaert & de Vriend (2003, 2010) have proposed a parameterization for the secondary flow that is valid over the entire curvature range. According to their parameterization, the magnitude of the secondary flow is obtained by adding a correction factor to linear model prediction:

$$\sqrt{\left\langle v_n^{*,2}\right\rangle} = \left[\frac{\sqrt{\left\langle f_n^2\right\rangle}}{\sqrt{\left\langle f_{n,0}^2\right\rangle}}(\mathcal{B})\right]\sqrt{\left\langle v_{n,0}^{*,2}\right\rangle} \tag{4}$$

The correction factor is represented by the term between square brackets. It depends uniquely on the so-called bend parameter $\mathcal{B}$, which is defined as:

$$\mathcal{B} = C_f^{-0.275}\left(H/R\right)^{-0.5}\left(\alpha_s + 1\right)^{0.25} \tag{5}$$

where U_s is the depth-averaged streamwise velocity, and α_s represents the normalized transverse gradient of U_s:

$$\alpha_s = \frac{R}{U_s}\frac{\partial U_s}{\partial n} \tag{6}$$

Because the magnitude of the secondary flow does not increase linearly with *H/R*, this parameterization is called a nonlinear model. Blanckaert & de Vriend (2003, 2010) have developed a cross-sectional-averaged model that determines the distribution of the depth-averaged velocity U_s, as parameterized by means of α_s, and the magnitude of the secondary flow expressed according to equation (3). Their model is computationally hardly more expensive than the commonly used linear models, but it is no longer restricted to mild and moderate curvatures. This model is able to resolve the aforementioned process of saturation of the secondary flow in sharply-curved open-channel reaches (Blanckaert 2009, Ottevanger 2012). Although the nonlinear model has been validated by Blanckaert & de Vriend (2003, 2010) and Ottevanger et al. (2013), further validation over an extended parameter space would enhance confidence in the model.

The first objective of the present paper is to contribute to the body of experimental data on the secondary flow in sharply curved open-channel reaches. The second objective is to investigate systematically the dependence of the secondary flow on two parameters: the curvature ratio *H/R* and the Froude number *Fr*. The third objective is to use the experimental data for assessment of the predictive capabilities of Blanckaert & de Vriend's (2003, 2010) nonlinear model.

2. THE EXPERIMENTS

A series of 18 experiments was performed in a 1.3 m wide open-channel laboratory flume, including a bend with an arc length of 193° and a constant radius of curvature of 1.7 m on the centreline. The bend was preceded by a 9 m long straight inflow reach, and followed by a 5 m long straight outflow reach. The bed consisted of quasi-uniform sand with a diameter of 0.002 m. the bed was transversally flat, but had a longitudinal slope of 0.003. Flow depth was controlled with an adjustable weir at the downstream end of the flume. Because the longitudinal water surface slope is not equal to the longitudinal bed slope in all experiments, flow depth slightly and gradually varied along the flume, resulting in quasi-uniform flow conditions.

Experiments were performed at flow depths of H = 0.09 m, 0.13 m, 0,19 m, and 0.26 m, corresponding to curvature ratios of *H/R* = 0.053, 0.077, 0.112 and 0.153, which range from moderately curved to very strongly curved flows. These flow depths were measured at the centreline in the cross-section at 75° in the bend. For each of these flow depths, experiments were performed at *Fr* = 0.1, 0.2, 0.3, 0.4, and 0.5. Because of limited pump capacity, experiments at *Fr* = 0.4 and 0.5 were not possible for the highest flow depth.

Non-intrusive velocity measurements were performed with an Acoustic Doppler Velocity Profiler (ADVP) on the centerline at 30°, 60°, 90°, 120°, 150° and 180° in the bend. The ADVP measures vertical profiles of the three-velocity components with high temporal and spatial resolution. Its working principle has been reported by Lemmin & Rolland (1997), Hurther & Lemmin (1998), and Blanckaert & Lemmin (2006). Measurements were made with a sampling frequency of 31.25 Hz and a sampling period of 60 s.

Water surface elevation measurements were performed with manual point gauges all around the flume, with a streamwise spacing of 1 m in the straight reaches and 15° in the curved reaches. The dimensionless Chézy friction coefficient was determined by fitting one-dimensional backwater curve computations to the measured water surface elevation.

3. RESULTS, DISCUSSION AND CONCLUSIONS

Figure 1(a) shows the pattern of the normalized transverse component of the secondary flow f_n (equation 1) measured in the streamwise-vertical plane along the centreline of the bend. The secondary flow comes into existence at the bend entry, grows in the first half of the bend and reaches a maximum magnitude near the cross-section at 90°, and subsequently decays towards the bend exit. Blanckaert (2009) has explained how the nonlinear interaction between the streamwise and secondary flow is at the origin of this evolution of the secondary flow around the bend. Figure (1b) shows the evolution of the normalized magnitude of the secondary flow (equation 2) around the bend. The experimental evolution is compared to predictions by the linear model of de Vriend (1977) and the nonlinear model of Blanckaert & de Vriend (2003, 2010). The linear model predicts a constant value around the bend, which is uniquely determined by C_f. The non-linear model closely agrees with the measured evolution around the bend. The bend-averaged values of the experimental data and the nonlinear model are quasi-identical, whereas the linear model considerably overpredicts the magnitude of the secondary flow. Figure (1c) compares the linear model prediction of f_n to the measured profiles. The measured profile is only close to the linear model prediction in the middle of the bend, where the secondary flow reaches its maximum magnitude. Elsewhere, the linear model considerably overpredicts the secondary flow.

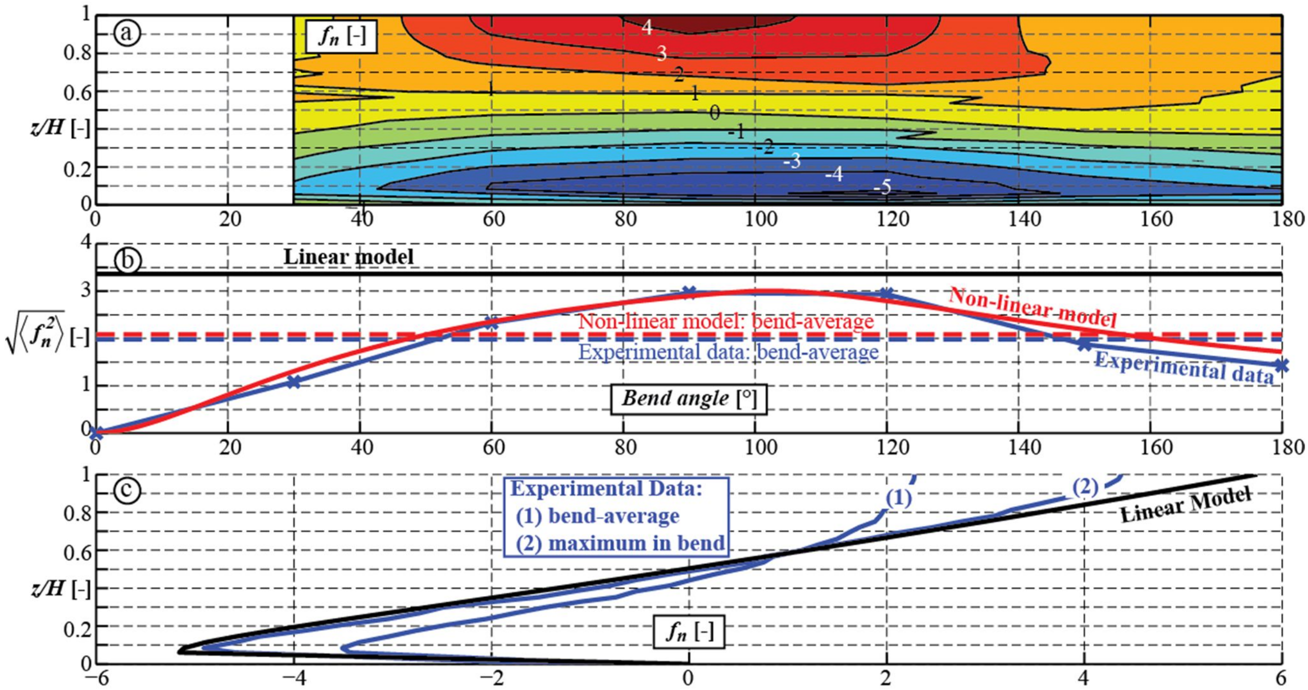

Figure 1. Results for the experiment with flow depth 0.13 m and Fr = 0.2. (a) Pattern of the measured normalized transverse component of the secondary flow f_n in the streamwise-vertical plane through the centreline. (b) Evolution of the magnitude of the secondary flow through the bend: experimental data, linear and nonlinear model predictions. (c) Normalized vertical profile f_n: maximum and average values in bend and linear model prediction.

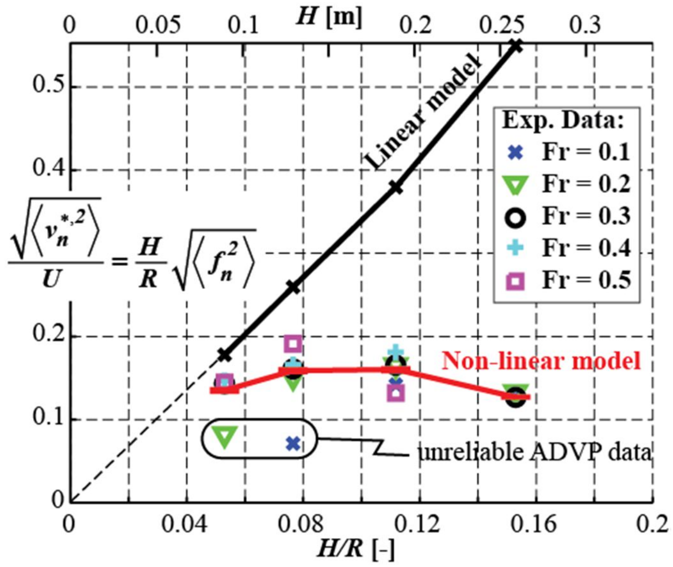

Figure 2. Bend averaged values of the normalized magnitude of the secondary flow in all 18 experiments: experimental data, linear and nonlinear model predictions.

Figure 2 summarizes the results for all 18 experiments. It compares the bend-averaged values of the normalized magnitude of the secondary flow computed from the experimental data to predictions by the linear and non-linear models. These results lead to the following observations and conclusions:

1) The linear model predicts a magnitude of the secondary flow that grows linearly with *H/R*. Slight deviations from the linear growth are due to slight variations in the dimensionless Chézy friction coefficient.
2) All experiments confirm that the secondary flow saturates in sharply curved open-channel flow. The normalized magnitude of the secondary flow remains about constant in all experiments.
3) The results do not show any dependence of the secondary flow on the Froude number. Differences between experiments with the same flow depth but different *Fr* are within the experimental uncertainty. The ADVP measurements were not successful for the experiments with flow depth of 0.09 m for *Fr* = 0.1 and 0.2, and flow depth of 0.13 m and *Fr* = 0.1. These failures can be attributed to the low velocities and associated low acoustic scattering levels.
4) The nonlinear model predictions agree very well with the experimental data in all experiments.

ACKNOWLEDGMENTS

The research was funded by the Sino-Swiss Science and Technology Cooperation, Institutional Partnership, grant numbers IP13_092011 and FU07-0302014.

REFERENCES

Blanckaert K. (2009), Saturation of curvature-induced secondary flow, energy losses, and turbulence in sharp open channel bends: Laboratory experiments, analysis, and modeling. *J. Geophys. Res.*, 114, F03015, doi:10.1029/2008JF001137.

Blanckaert K., and de Vriend H.J. (2003). Nonlinear modeling of mean flow redistribution in curved open channels. *Water Resour. Res.*, 39(12), 1375–1388.

Blanckaert K., and de Vriend H.J. (2004). Secondary flow in sharp open-channel bends. *J. Fluid Mech.*, 498, 353–380.

Blanckaert K., and de Vriend H.J. (2010). Meander dynamics: A nonlinear model without curvature restrictions for flow in open-channel bends. *J. Geophys. Res.*, 115, F04011, doi:10.1029/2009JF001301.

Blanckaert K., and Lemmin U. (2006). Means of noise reduction in acoustic turbulence measurements. *J. Hydraul. Res.*, 44(1), 3–17.

de Vriend H.J. (1977). A mathematical model of steady flow in curved shallow channels. *J. Hydraul. Res.* 15(1), 37– 54.

Engelund F. (1974). Flow and bed topography in channel bends. *J. Hydraul. Div.*, 100(HY11), 1631-1648.

Fargue L. (1868), Étude sur la corrélation entre la configuration du lit et la profondeur d'eau dans les rivières á fond mobile. *Annales Des Ponts Et Chaussées*, 38, 34–92 (in French).

Hurther D., and Lemmin U. (1998). 'A constant beamwidth transducer for three-dimensional Doppler profile measurements in open channel flow. *Measurement Science and Technology*, 9(10), 1706–1714.

Johannesson H., and Parker G. (1989). Secondary flow in a mildly sinuous channel. *J. Hydraul. Eng.*, 115(3), 289–308.

Lemmin U., and Rolland T. (1997). Acoustic velocity profiler for laboratory and field studies. *J. Hydr. Eng.*, 123(12), 1089–1098.

Ottevanger W. (2013). Modelling and parameterizing the hydro- and morphodynamics of curved open channels. PhD Thesis, Delft University of Technology, Delft, The Netherlands.

Ottevanger W., Blanckaert K., and Uijttewaal W.S.J. (2012). Processes governing the flow distribution in sharp river bends. *Geomorphology*, 163-164, 45-55..

Rozovskii I.L. (1957). Flow of water in bends of open channels. Academy of Sciences of the Ukrainian SSR, Kiev, 1957; Israel Program for Scientific Translations, Jerusalem, 1961.

Thomson W. (1876). On the origin of windings of rivers in alluvial plains, with remarks on the flow of water round bends in pipes. *Proc. R. Soc. Lond.* 25, 5–8.

van Bendegom L. (1947). Eenige beschouwingen over riviermorphologie en rivierverbetering. *De Ingenieur*, 59(4), 1-11 (in Dutch).